METALS AND MATERIALS International, Vol. 7, No. 5 (2001), pp. 413~420

Developing SPD Methods for Processing Bulk Nanostructured Materials with Enhanced Properties

R. Z. Valiev

Institute of Physics of Advanced Materials, Ufa State Aviation Technical University
12 K. Marx St., Ufa, 450000, Russia

Severe plastic deformation (SPD), i.e. intense plastic straining under high pressure, is an innovative technique for processing ultrafine-grained nanostructured metals and alloys. SPD fabricated nanostructures can lead to novel properties, which, however, depend strongly on the processing parameters. This paper focuses on examples of attaining enhanced mechanical properties in several metals and alloys, subjected to severe plastic deformation. In addition, the relationships among the processing conditions, microstructures and properties of the materials produced by SPD are considered.

Keywords : severe plastic deformation, bulk nanomaterials, enhanced properties

1. INTRODUCTION

Strong refinement of the microstructure and formation of nanostructures in bulk metallic materials through severe plastic deformation (SPD) provides the potential to achieve new and extraordinary properties for these materials [1,2]. This is not only because of the unique physical and mechanical properties inherent in various nanostructured materials, e.g. by inert gas condensation processing [3,4] or ball milling with subsequent consolidation [5], but also because of several advantages of SPD materials over other nanomaterials. In particular, SPD methods have resulted in overcoming a number of difficulties connected with residual porosity in compacted samples, impurities from ball milling, the processing of large scale billets and the practical application of the given materials. However, attaining advanced properties is a complex problem, because, as is well established [6] for nanostructured SPD materials it is typical of them to have not only very small grain sizes, but also specific defect structures, high internal stress, crystallographic texture, and often a change of phase composition. All these microstructural parameters are important in attaining enhanced properties. This is why the relationship between the microstructures and enhanced properties in SPD-fabricated materials has become an intense investigative objective. This paper presents several examples illustrating how unique and advanced properties can be obtained in metals and alloys through SPD-induced microstructures.

2. INVESTIGATION AND DEVELOPMENT OF SPD PROCESSING

High pressure torsion (HPT) (Fig. 1(a)) and equal-channel angular (ECA) pressing (Fig. 1(b)) refer to methods used in pioneer work devoted to ultrafine-grained (UFG) structure formation in metals and alloys [7,8] as a result of large deformations with a true strain of 10 and more without damage to samples. These methods have recently been further developed.

2.1. High pressure torsion

Recent investigations have demonstrated, in particular, the ability to produce homogeneous nanostructures with a grain size of about 100 nm and less having high-angle grain boundaries by means of HPT [2,6,9]. This method may therefore be considered a new technique for bulk nanostructured materials processing.

Samples processed under high pressure torsion deformation are disk-shaped (Fig. 1(a)). In this process the sample is put between anvils and compressed under pressure (P) in several GPa. Lower anvil turns and friction forces bring about the shear straining of the sample. As a result, the deformed sample does not break despite high deformation strain.

Essential structure refinement is observed after half- or one- complete (360^{o}) turn deformation. But to create homogeneous nanostructure deformation several turns are necessary (Fig. 2). The important role of applied pressure

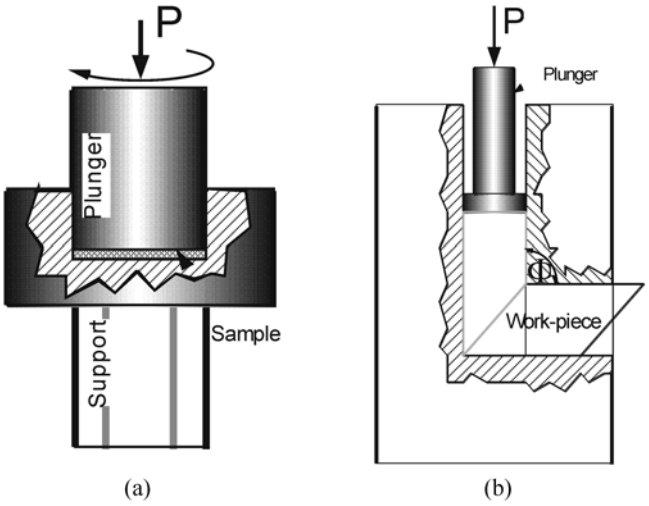

Fig. 1. Severe plastic deformation technique principles: (a) high pressure torsion and (b) ECA pressing.

in the formation of a homogeneous nanostructured state in Ni during the HPT process is shown in the recent work [10].

HPT has been successfully applied in the microstructure refinement of metals, alloys and, recently, in composites and semiconductors [6]. The important advantage of this technique is the possibility of adjusting the cumulative strain, applied pressure and deformation speed. This possibility makes HPT a very convenient technique for the investigation of the influence of different parameters on structure and properties evolution during SPD. We must note, however, that samples processed with HPT are of small-size. The topical problem is the enlargement of their size. Another important problem is the increase in the microstructure homogeneity of the HPT samples. This is connected with the different cumulative strains in the center and periphery of the samples.

2.2. ECA pressing

In the early 1990s ECA pressing [11] was developed and applied for the first time as an SPD technique for the processing of microstructures with submicro- and nanometer grain sizes [7,8]. In these early experiments, original ingots with square or round cross sections were cut out of rods with lengths of from 70 up to 100 mm. The diameter of their cross section or their diagonal did not exceed 20 mm.

During ECA pressing implementation, the ingot is pressed in a special die through two channels with equal cross sections intercrossing, as usual, at an angle of 90^{o} (Fig. 1(b)). In the case of hard-to-deform materials, the deformation is realized at elevated temperatures or with extended channels crossing angles if important. There are also some particular requirements about heat resistance and die durability. Each pass conforms to the supplementary strain, approximately 1, for the most often applied channels crossing angle, 90^{o}.

Strong microstructure refinement with the ECA pressing technique can quite easily be processed both in pure metals and in alloys. However, the fabrication of homogeneous UFG nanostructures having high-angle grain boundaries with the ECA pressing technique is a complex problem. It is well-known that the number of passes and the selected ECA pressing route are very important parameters in the processing.

The influence of the number of passes (cumulative strain) and of the ECA pressing routes on microstructure evolution for a number of metals and alloys, namely Al-Mg alloys [12], and pure Ti [13], was investigated in detail. It was shown that homogeneous microstructure in alloys can be observed just after 4-6 passes, following the route B_C. During this process a billet turned between consecutive passes in one direction around its axis with an angle of 90^{o}. Analysis of the shearing characteristics for different processing routes indicates that route B_C leads to the rebuilding of the shape of the initially cubic element in the unpressed sample after 4n and 2n (n - an integer) passes through the die and leads to homogeneous equiaxed structure formation [12].

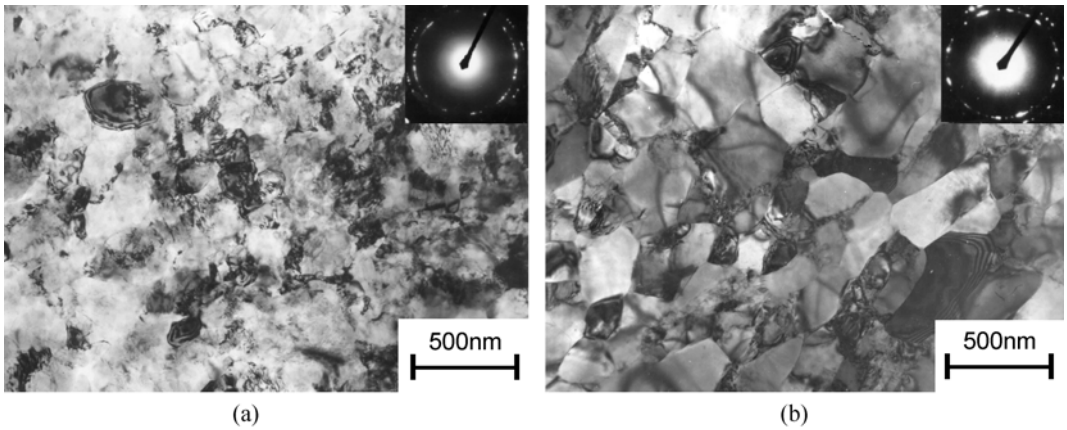

Fig. 2. TEM images of UFG Cu formed by (a) HPT and (b) ECA pressing.

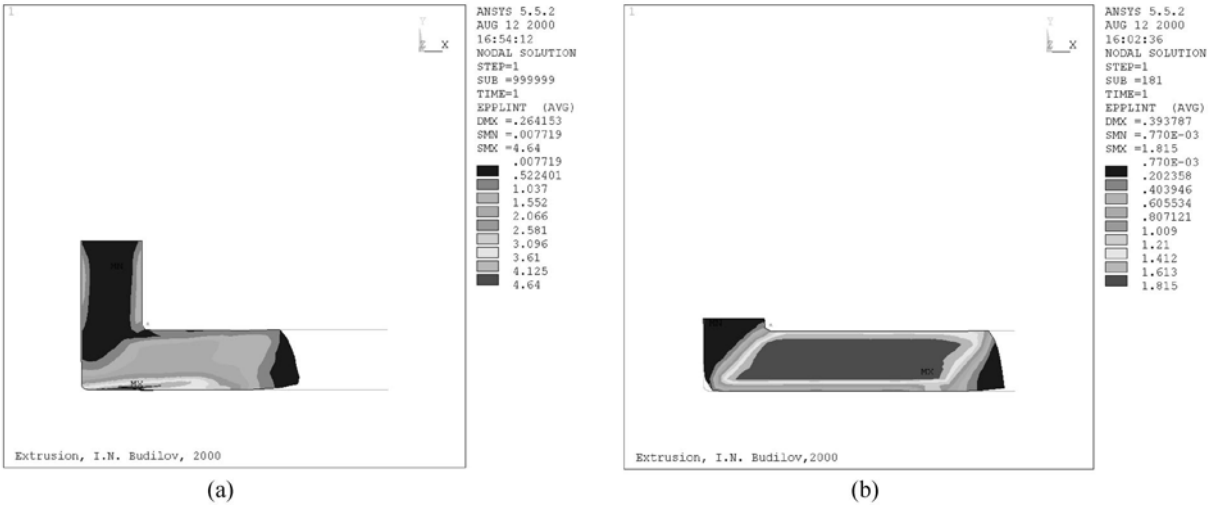

Fig. 3. The distribution of plastic deformations intensity in the case of different friction coefficient k values: (a) k=0.2 and (b) k=0 [15].

According to similar investigations on Ti it is preferable also to follow the route B_C in order to form equiaxed grain structure and higher ingot shape and surface quality [13].

The experimental and theoretical modelling of the mechanics of ECA pressing, e.g. the stress-deformed state and the contact stresses in the die, is one of the important tasks in developing SPD processing. Investigations on the friction coefficient influence between the deforming billet and die-walls and the determination of the contact stress in the die-walls have shown [14,15] that the shear plastic strain during ECA pressing could be essentially non-uniform along the deformed sample. At the same time, the significant sensibility of the plastic deformation uniformity to the friction conditions between the ingot and die has been found (Fig. 3) [15]. The approaches to the enhancement of ECA pressing uniformity due to the optimization of friction conditions based on the results obtained from experimental and FEM have been worked through. On this basis a die was fabricated and bulk billets with uniform ultrafine-grains in hard-to-deform Ti were obtained [15]. Here a maximum ingot size of up to 60 mm in diameter and 200 mm in length (Fig. 4) was reached.

Fig. 4. Bulk Ti billets, processed by ECA pressing.

3. FUNDAMENTAL PARAMETERS

At present it has already been established that many fundamental properties undergo significant changes in nanostructured SPD materials similar to nanocrystals processed by other techniques [3,5]. Among these properties, the most interesting are changes in the Curie and Debye temperatures and saturation magnetization, which are commonly structure insensitive and usually reflect changes occurring in the atomic crystal structure of solids. Another example is the change in elastic properties which are determined by inter-atomic interactions as well.

The values of some fundamental parameters of nanostructured SPD materials in comparison with coarse-grained analogues are given in Table 1.

It can be seen that the formation of nanostructures leads to changes in fundamental magnetic characteristics such as the Curie temperature and saturation magnetization. Although these properties are characteristic of ferromagnetic materials, they reflect features of the nanostructured state. For example, investigations of nanostructured nickel with a mean grain size of 20 nm which was processed by SPD consolidation of ball-milled powder, revealed quite significant changes in magnetic characteristics [16].

Significant changes were revealed also in the value of the Debye temperature which was measured by means of X-ray methods (see [6] for details) and Mössbauer spectroscopy [17]. The decrease revealed in the Debye temperature manifests an increase in the dynamic properties of the atoms which are attributed to changes in the diffusion coefficient as well. As an example, the data for the diffusion coefficient of

Table 1. Some fundamental properties of metals in nanostructured (NS) and coarse-grained (CG) states

Properties	Materials	Value		Reference
		NS	CG	
Curie temperature, K	Ni	595	631	[16]
Saturation magnetization, Am^2/kg	Ni	38.1	56.2	[16]
Debye temperature, K	Fe	240*	467	[17]
Diffusion coefficient, m^2/s	Cu in Ni	1×10^{-14}	1×10^{-20}	[18]
Ultimate solubility at 293 K, %	C in α-Fe	1.2	0.06	[23]
Youngs modulus, GPa	Cu	115	128	[22]

*for near boundary regions

copper in nanostructured nickel are presented in Table 1. In [18] experiments on the determination of the depth of copper penetration into nickel were conducted by means of secondary ion mass-spectroscopy. Comparative diffusion experiments were carried out at temperatures of 423 K and 523 K for 3 hours using ECA-pressed nanostructured and coarse-grained nickel. Under given conditions, copper atoms were not detected in the coarse-grained nickel even at a depth of 2 mm. At the same time, the diffusive copper fluxes in nanostructured nickel penetrated to a depth greater than 25 and 35 mm at 423 and 573 K, respectively. The calculation of the grain-boundary diffusion coefficients of copper in nanostructured nickel were based on these data. These experimental data demonstrate an increase in the grain boundary diffusion coefficient of copper in nanostructured nickel in comparison with coarse-grained nickel. According to the data presented in [18], this difference is of 4-6 orders.

The enhanced diffusivity and permeability of the grain boundaries which was revealed also in other nanostructured SPD materials [19,20] is important evidence for a specific structure in their boundaries, suggesting their enhanced free volume, excess energy and long range stresses [21].

Among other parameters, changes in which are attributed to the nanostructured SPD state, are the elastic moduli and ultimate solubility of carbon in α-Fe (Table 1). The measurements of ultra sound velocities obtained were used to calculate the elastic moduli, which as compared to coarse-grained copper, were lower by 10-15% [22]. It was assumed that the overall moduli of a nanostructured material could be combinations of the elastic moduli of the matrix and of the near grain boundary region, which is about 50% of the value of the elastic modulus in coarse-grained metal.

Thus, the recent investigations demonstrate a number of anomalies in the fundamental characteristics of nanostructured SPD materials. These changes are obviously associated not only with small grain size but also with the specific defect structure of non-equilibrium grain boundaries.

4. MECHANICAL PROPERTIES AND BEHAVIOUR

Another important sphere of research which has been developing intensively in recent years is the investigation of the mechanical properties of nanostructured materials. In terms of mechanical properties, the formation of nanostructures in various metals and alloys should lead to high strength in these materials according to the well-known Hall-Petch relationship [24] and the occurrence of low temperature and/or high strain rate superplasticity [25,26]. The great interest in the physics of the strength and plasticity of ultrafine-grained materials is conditioned by a possible change in the mechanisms of plastic deformation since, according to theoretical estimates, the initiation and movement of dislocations may become impossible in grains of a nanometric size [24,27]. In terms of practical application, one can expect the engineering of new advanced high-strength materials and the achievement of enhanced superplastic properties.

The fabrication of such bulk fully dense nanostructured materials by means of SPD methods provided an opportunity to start systematic studies of their mechanical properties [26,28].

4.1. Strength at room temperature

As an example, SPD copper was used recently for mechanical tests in [29,30]. Fig. 5 shows the "true stress-strain" curves of the Cu specimens processed by ECA pressing tested for compression and tension at room temperature. For comparison, similar curves are given for annealed specimens. It may be seen (Fig. 5(a)) that ultrafine-grained Cu with a grain size of about 200 nm has a yield strength that is several times higher and reveals low strain hardening in contrast to coarse-grained annealed Cu having a mean grain size of 30 μm.

The stress-strain curve for a specimen subjected to additional annealing at 473 K for 3 min is shown in Fig. 5(b). This annealing does not cause noticeable grain growth but leads to an abrupt decrease in the level of internal stress due to the recovery of dislocations at the grain boundaries [29]. It

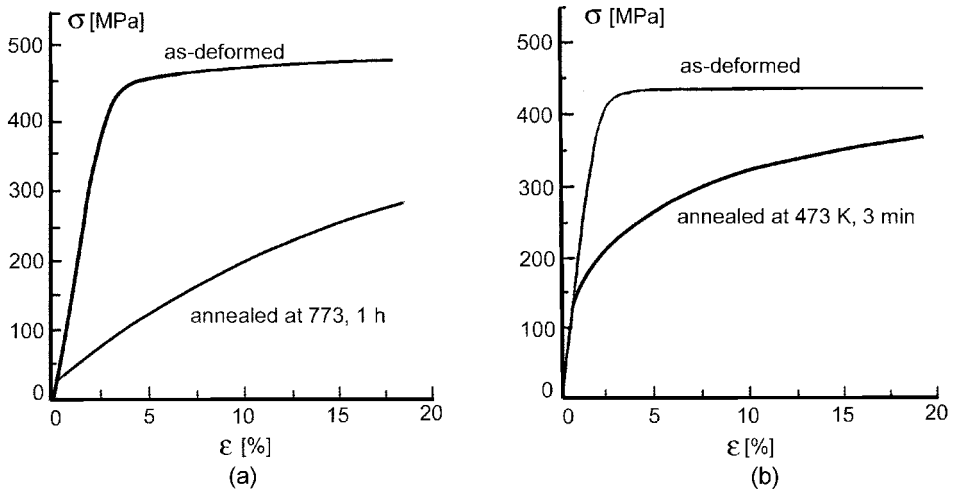

Fig. 5. "True stress strain" curves of SPD Cu at room temperature (a) tension and (b) compression.

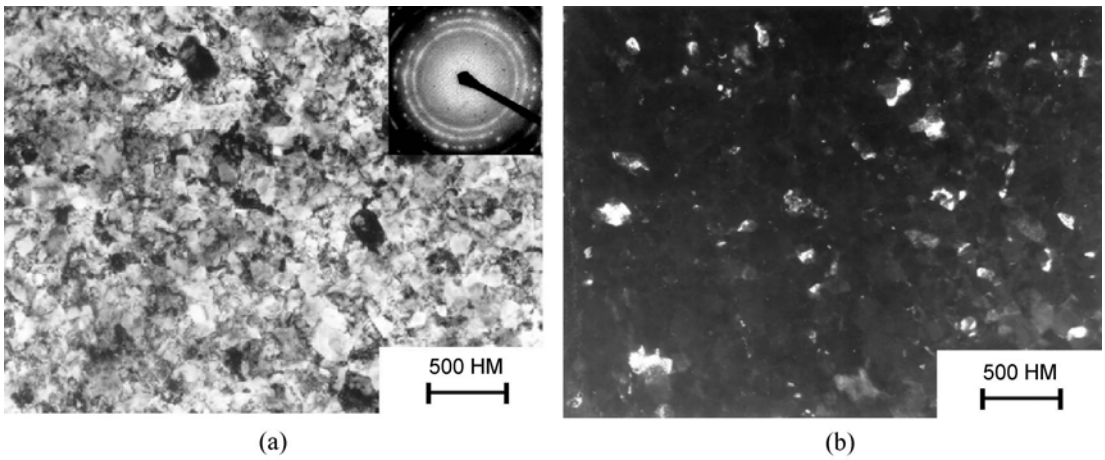

Fig. 6. Microstructure of the Cu+0.5 wt.%Al_2O_3 composite (type D): (a) bright field image and (b) dark field image from spot 111 of Cu.

can be seen that, despite similar grain sizes, the specimens in these two states substantially differ in deformation behaviour. The shape of the curve for the specimen subjected to such short-term annealing is similar to that of coarse-grained copper. This illustrates that the strength of SPD materials is affected not only by grain size, but also by grain-boundary defect density which can be changed by some annealing. The application of HPT to the Cu+0.5%Al_2O_3 composite can lead to the fabrication of very small grains having an average size of about 80 nm (Fig. 6) [31]. Such a composite demonstrates the advanced combination of high strength and ductility during tensile tests at room temperature (Fig. 7). Similar behaviour was observed recently in nanostructured SPD Ti as well [32].

As was already mentioned, structure refinement in SPD alloys may accompany substantial changes in phase composition. The latter phenomenon can also be quite important for mechanical properties. For example, the aging behaviour of the aluminum alloys Al 1420 [6] and Al-11% Fe [33] after high pressure torsion is considered below.

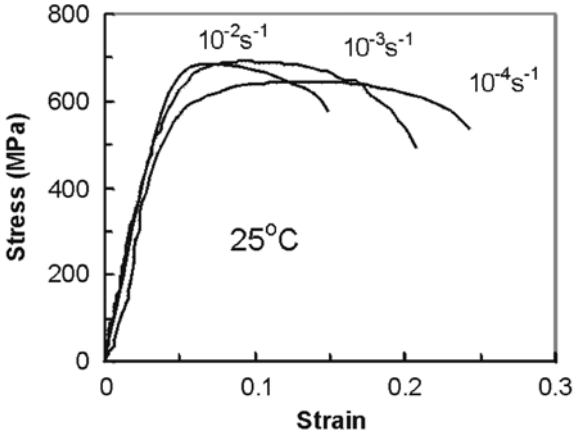

Fig. 7. Tensile stress-strain curves for the Cu+0.5%Al_2O_3 nanocomposite with grain size of 80 nm tested at room temperature at strain rates of 10^{-2}, 10^{-3}, 10^{-4} s^{-1}.

To obtain a high-strength state, the alloy Al 1420 (Al-5.5%

Table 2. Microhardness of aluminum alloys (MPa)

Treatment	Alloy	
	Al 1420	Al-11wt.%Fe
Initial state	540	710
After severe deformation	1750	1700
After SPD and aging	2300	3020

Mg-2.2% Li-0.12% Zr) was sequentially quenched, severely deformed by torsion, and aged at 120°C. This aging temperature was selected to ensure additional precipitation with retention of small grain size. The microhardness of the as-quenched alloy was 540 MPa (Table 2). The severe torsion of this alloy caused the formation of a nanostructure with a mean grain size of 70 nm.

SPD increases microhardness to 1750 MPa. Aging at 120° C retains the average grain size of 70 nm but causes precipitation of second-phase particles with a size of about 20 nm and an increase in microhardness up to 2300 MPa.

A similar effect was seen in Al-11wt.%Fe alloy whose structure and aging behaviour was studied in detail in [33]. The microhardness of the SPD alloy is 1700 MPa and substantially increases after annealing at 100°C for 5 h (Table 2) due to the intense aging of the alloy. This shows that the formation of nanostructures in Al alloys is accompanied by the formation of metastable oversaturated solutions whose decomposition during aging causes a substantial strengthening of the alloys.

4.2. Fatigue behaviour

The formation of nanostructures with SPD processing may have a substantial effect on the fatigue behaviour of metals and alloys as well. For example, the cyclic strengthening of four copper specimens was studied in [34]. Two specimens were taken in the as-ECA pressed state, and two other specimens were additionally subjected to short-term annealing (473 K, 3 min), which retains the grain size, or to annealing at 773 K, which causes substantial grain growth (up to 50 mm). All specimens exhibited saturation after several cycles, but the value of the saturation stress s_s is greatly affected by the preliminary treatment of copper (Fig. 8).

A substantial difference in the fatigue behaviour of ultrafine-grained and coarse-grained copper was established from the dependence of the hysteresis loss parameters (Bauschinger-energy parameter) B_E as a function of accumulated plastic deformation as well. The B_E value was estimated from the shape of the hysteresis loop. The larger the value of B_E, the more pronounced is the Bauschinger effect. As was shown, the B_E value for all states is little affected by the accumulated deformation, but a maximum B_E value is observed for the SPD copper subjected to short-term annealing. Thus, the results of [34] indicate that SPD materials can have unusual

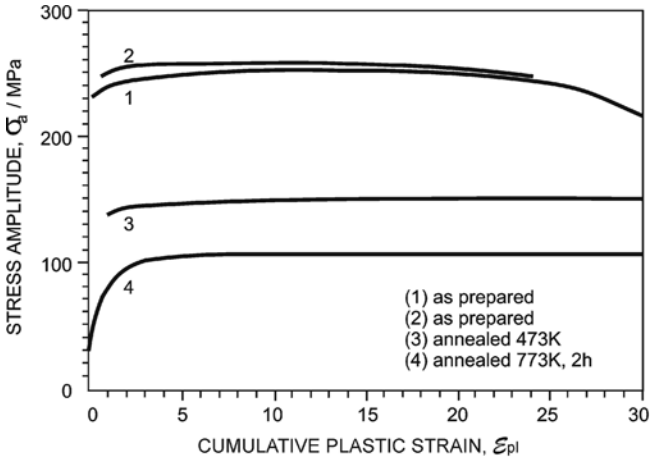

Fig. 8. Fatigue behaviour of nanostructured copper: curve of cyclic strengthening.

fatigue properties. The higher fatigue strength of SPD Cu demonstrated the fact that its B_E value is smaller than that of the specimen additionally subjected to short-term annealing.

Note should be made that quite recently it was shown [35] that Cu after ECA pressing can also demonstrate cycling softening for the same test conditions. The reason for this is, obviously, microstructural non-homogeneity during the process of ECA pressing in non-optimal regimes and microstructure instability at cyclic loading.

4.3. Superplasticity

In recent years several studies were devoted to further researching the unusual superplastic properties of SPD nanostructured alloys at elevated temperatures. The earliest work investigating superplasticity in SPD alloys already showed the possibility of considerable enhancement of their properties. In [26], grain size of 150 nm was obtained in the Al-4% Cu-0.5% Zr alloy by ECA pressing. This material contains ultrafine Al_3Zr particles of 30 nm in size. These specimens tested by tension at 250°C at strain rates ranging from 2.8×10^{-5} to 1.4×10^{-3} s^{-1} exhibit very high elongation to failure, despite a relatively low test temperature. A maximum elongation (850%) was obtained at a starting strain rate of 1.4×10^{-3} s^{-1}. The strain-rate sensitivity m in this case is 0.46. Note that the same alloy with a grain size of 8 μm exhibits similar superplastic behaviour only at temperatures as high as 500°C. This example illustrates superplasticity in SPD materials at relatively low temperatures.

Another unusual effect is the high strain rate superplasticity recently revealed in Al-based alloys 1420 (Al-5.5% Mg-2.2% Li-0.12% Zr) subjected to ECA pressing [36]. The grain size of the investigated alloys was about 1 mm and the grain boundaries are mostly high-angle. Mechanical tests showed that this material had very high superplastic properties. Thus, the elongation to failure of the specimens tested at

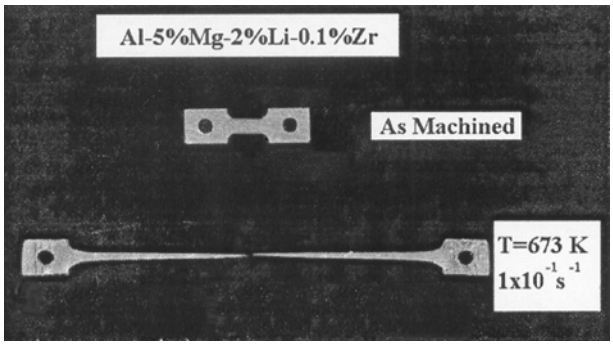

Fig. 9. Appearance of the Al 1420 alloy processed by ECA pressing before and after a tensile test at 400°C with a strain rate of 10^{-1} s^{-1}.

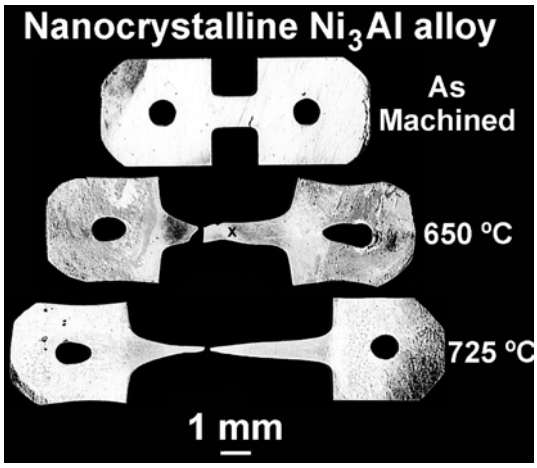

Fig. 10. Appearance of nanostructured Ni_3Al samples prior to and after tension at temperature 650°C, 1×10^{-3}, elongation 390% (a cross indicates the place where the foil was cut out for HREM/TEM) and at temperature 725°C, 1×10^{-3}, elongation 560%.

350°C at a strain rate of 10^{-2} s^{-1} is 1180%. Moreover, the specimens demonstrate superplastic behaviour even at a strain rate of 10^{-1} s^{-1}, exhibiting elongation of about 1000% (Fig. 9). These results are the first evidence of the high-strain-rate superplasticity of commercial cast Al alloys subjected to SPD processing. The effect of high strain rate superplasticity has been already demonstrated in several other SPD alloys [36,37].

Another material with unique superplastic properties is the $Ni_3Al(Cr)$ intermetallic alloy with an addition of 0.1 wt.% B [38]. High pressure torsion causes disordering of this alloy and an average grain size of 50 nm in the as-deformed alloy is retained after annealing at temperatures as high as 650°C. Tensile tests showed that at 650°C and 725°C, this nanocrystalline intermetallic compound exhibits superplastic behaviour; i.e., its elongation to failure at a strain rate of $10^{-3}s^{-1}$ is about 390% and 560%, respectively [38,39]. This phenomenon is rather unusual, because this alloy with micron-scale grain size is known to exhibit superplastic behaviour at the substantially higher temperature of 1150°C. The data obtained are also of great importance in the context of superplastic forming at the relatively low temperatures of complex shape articles from intermetallic compounds which are usually very brittle.

At 650°C, nanostructured Ni_3Al revealed a superplastic behaviour and the appearance of an Ni_3Al specimen after testing is shown in Fig. 10 in which the upper specimen is the untested one. It is apparent from Fig. 10 that the specimens exhibit very high tensile ductilities (several hundred percent elongation to failure) without visible macroscopic necking. This confirms the manifestation of superplastic behaviour at quite low temperatures. However, this superplasticity is associated with considerable strain hardening, which leads to high strength.

In order to understand the mechanisms of unusual superplasticity in this nanostructured alloy, special TEM/HREM investigations of a thin foil prepared from a gauge section of the Ni_3Al sample strained about 300% (see Fig. 10) was performed. Although there is some grain growth during superplastic deformation, the grain size remained less than 100 nm [41]. Grains were not elongated and there was no evidence of any considerable dislocation activity inside the grains even though careful HREM investigations were conducted as well. This experiment supports the theoretical calculations demonstrating the difficulty of accommodation for grain boundary sliding through generation of lattice dislocations in nanograins during superplastic deformation [40]. Probably the superplastic deformation of nanomaterials occurs as a result of grain boundary sliding and some diffusional accommodation without visible dislocation activity in the grains.

5. SUMMARY AND CONCLUSIONS

The examples given of recent investigations indicate that SPD-fabricated nanostructures can lead to novel properties, both physical and mechanical. The observed changes in Curie and Debye temperatures, saturation magnetization, elastic moduli, which are typically microstructure insensitive and usually reflect changes in the atomic and electronic structure of solids, are of special interest. Variation in other fundamental parameters, i.e. diffusivity, solubility limit has also been revealed in several SPD-processed metals and alloys. In terms of practical application, it is important that the mechanical behaviour of ultrafine-grained SPD materials is often characterized by such advanced properties as high strength and ductility, high fatigue properties and enhanced superplasticity. However, these properties are originated by either very small grain sizes and a specific defect structure. To enhance properties the microstructure of SPD processed materials must be carefully characterized and controlled. Thus, the establishment of SPD processing guidelines has

become topical in order to obtain new advanced properties in metallic materials.

ACKNOWLEDGMENT

The author gratefully acknowledges numerous discussions and cooperation with Profs A.K. Mukherjee, T.G. Langdon, T.C. Lowe, I.V. Alexandrov and other students and colleagues, mentioned in our joint publications. This work was supported in part from the EU INTAS projects #991216, 1741.

REFERENCES

1. R. Z. Valiev, *Ann. Chim. Fr.* **21**, 269 (1996).
2. R. Z. Valiev, *Proc. of the NATO ARW on Investigation and Applications of Severe Plastic Deformation: NATO Sci. Series* (eds., T. C. Lowe and R. Z. Valiev), p. 80, Kluwer Pub., Moscow, Russia (2000).
3. H. Gleiter, *Prog. Mater. Sci*. **33**, 223 (1989).
4. J. R. Weertman, *Mater. Sci. Eng. A* **166**, 161 (1993).
5. D. G. Morris, *Mechanical Behaviour of Nanostructured Materials*, p. 85, Trans Tech. Pub., Switzerland (1998).
6. R. Z. Valiev, R. K. Islamgaliev and I. V. Alexandrov, *Prog. Mater. Sci*. **45**, 102 (2000).
7. R. Z. Valiev, A. V. Korznikov and R. R. Mulyukov, *Mater. Sci. Eng. A* **186**, 141 (1993).
8. R. Z. Valiev, N. A. Krasilnikov and N. K. Tsenev, *Mater. Sci. Eng. A* **137**, 35 (1991).
9. R. Z. Valiev, Y. V. Ivanisenko, E. F. Rauch and B. Baudelet, *Acta mater.* **44**, 4705 (1996).
10. A. P. Zhilyaev, S. Lee, G. V. Nurislamova, R. Z. Valiev and T. G. Langdon, *Scripta mater.* (2001), in press.
11. V. M. Segal, V. I. Reznikov, A. E. Drobyshevskiy and V. I. Kopylov, *Russian Metallurgy* **1**, 99 (1981).
12. T. G. Langdon, M. Furukawa, M. Nemoto and Z. Horita, *JOM* **52**, 30 (2000).
13. V. V. Stolyarov, Y. T. Zhu, I. V. Alexandrov, T. C. Lowe and R. Z. Valiev, *Mater. Sci. Eng. A* **299**, 59 (2001).
14. I. V. Alexandrov and R. Z. Valiev, *Scripta mater.* (2001), to be published.
15. V. S. Zhernakov, I. N. Budilov, G. I. Raab, I. V. Alexandrov and R. Z. Valiev, *Scripta mater.* (2001), to be published.
16. R. Z. Valiev, G. F. Korznikova, K. Y. Mulyukov, R. S. Mishra and A. K. Mukherjee, *Phil. Mag. B* **75**, 803 (1997).
17. R. Z. Valiev, R. R. Mulyukov, V. V. Ovchinnikov and V. A. Shabanov, *Scripta metall. mater.* **12**, 25 (1991).
18. Y. R. Kolobov, G. R. Grabovetskaya, Z. Z. Zratochka, E. R. Kabanova, E. V. Naidenkin and T. C. Lowe, *Ann. Chim. Sci. Mater.* **21**, 483 (1996).
19. R. Z. Valiev, I. M. Razumovskii and V. I. Sergeev, *Phys. Stat. Sol. A* **139**, 321 (1993).
20. R. Würschum, A. Kubler, S. Gruss, P. Acharwaechter, W. Frank, R. Z. Valiev, R. R. Mulyukov and H. E. Schaeffer, *Ann. Chim. Sci. Mater.* **21**, 471 (1996).
21. R. Z. Valiev, *Nanostruct. Mater.* **6**, 73 (1995).
22. N. A. Akhmadeev, N. P. Kobelev, R. R. Mulyukov, Y. M. Soifer and R. Z. Valiev, *Acta metall. mater.* **41**, 1041 (1993).
23. A. V. Korznikov, Y. V. Ivanisenko, D. V. Laptionok, I. M. Safarov, V. P. Pilyugin and R. Z. Valiev, *Nanostruct. Mater.* **4**, 159 (1994).
24. J. R. Weertman, *Mater. Sci. Eng. A* **166**, 161 (1993).
25. A. H. Chokshi, A. K. Mukherjee and T. G. Langdon, *Mater. Sci. Eng. R* **10**, 237 (1993).
26. R. Z. Valiev, *Mater. Sci. Forum* **243-245**, 207 (1997).
27. V. G. Gryaznov and L. I. Trusov, *Prog. Mater. Sci.* **37**, 289 (1993).
28. R. Z. Valiev, T. C. Lowe and A. K. Mulherjee, *JOM* **52**, 36 (2000).
29. V. Y. Gertsman, R. Z. Valiev, N. A. Akhmadeev and O. V. Mishin, *Mater. Sci. Forum*. **233**, 80 (1996).
30. R. Z. Valiev, E. V. Kozlov, Y. F. Ivanov, J. Lian, A. A. Nazarov and B. Baudelet, *Acta metall. mater.* **42**, 2467 (1994).
31. I. V. Alexandrov, Y. T. Zhu, T. C. Lowe, R. K. Islamgaliev and R. Z. Valiev, *Metall. Mater. Trans. A.* **29**, 2253 (1998).
32. A. A. Popov, I. Y. Pyshmintsev, S. L. Demakov, A. G. Illarionov, T. C. Lowe, A. V. Sergeeva and R. Z. Valiev, *Scripta mater.* **37**, 1089 (1997).
33. O. N. Senkov, F. H. Froes, V. V. Stolyarov, R. Z. Valiev and J. Liu, *Scripta mater*. **38**, 1511 (1998).
34. A. Vinogradov, Y. Kaneko, K. Kitagawa, S. Hashimoto, V. V. Stolyarov and R. Z. Valiev, *Scripta mater.* **36**, 1345 (1997).
35. S. R. Agnew and J. R. Weertmann, *Mater. Sci. Eng. A* **244**, 145 (1998).
36. R. Z. Valiev, A. D. Salimonenko, N. K. Tsenev, P. B. Berbon and T. G. Langdon, *Scripta Mater.* **37**, 724 (1997).
37. S. Komura, P. B. Berbon, M. Furukawa, Z. Horita, M. Nemoto and T.G. Langdon, *Scripta Mater.* **38**, 1851 (1998).
38. R. S. Mishra, R. Z.Valiev, S. X. McFadden and A. K. Mukherjee, *Mater. Sci. Eng. A* **252**, 174 (1998)
39. S. X. McFadden, R. S. Mishra, R. Z. Valiev, A. P. Zhilyaev and A. K. Mukherjee, *Nature* **398**, 984 (1999).
40. R. Z. Valiev, C. Song, S. X. McFadden, A. K. Mukherjee and R. S. Mishra, *Phylos. Magazine A* **81**, 25 (2001).
41. R. S. Mishra and A. K. Mukherjee, *Superplasticity and Superplastic Forming* (eds., A. K. Ghosh and T. R. Bieler), p. 109, TMS (1998).